ToF-SIMS analysis of abiotic and biotic iron sulfide layers formed in aqueous conditions on iron surfaces

Anne-Ilham El Menjra, Antoine Seyeux, Dimitri Mercier, Iwona Beech, Zakari Makama, Philippe Marcus

ToF-SIMS analysis of abiotic and biotic iron sulfide layers formed in aqueous conditions on iron surfaces

Anne-Ilham El Menjra[a], Antoine Seyeux[a,*], Dimitri Mercier[a], Iwona Beech[b,c], Zakari Makama[b], Philippe Marcus[a,*]

[a] PSL Research University, CNRS-Chimie ParisTech, Institut de Recherche de Chimie Paris/ Physical Chemistry of Surfaces Group, 11 rue Pierre et Marie Curie, 75005 Paris, France

[b] Department of Microbiology and Plant Biology, University of Oklahoma, Norman, OK, United States

[c] Center for Biofilm Engineering, Montana State University, Bozeman, MT, USA

*corresponding authors: antoine.seyeux@chimieparistech.psl.eu , philippe.marcus@chimieparistech.psl.eu

Abstract

An approach for the identification of the origin of iron sulfides formation on iron surfaces using Time-of-Flight Secondary Ions Mass Spectrometry (ToF-SIMS) is reported here in.

Two different sulfidation processes of iron surfaces are presented (both at room temperature): the first abiotic procedure was carried out using chronoamperometry (E = -0.8 V/SCE) of pure iron in 10 mM of $Na_2S,9H_2O$ (pH =11) while the second biotic procedure was accomplished by immersing a pure iron sample in a medium containing HS^- ions produced by a sulfate-reducing bacterium (SRB) of the genus *Desulfovibrio* at an open circuit potential (OCP). A surface analytical method using Time-of-Flight Secondary Ions Mass Spectrometry (ToF-SIMS) coupled with ToF-SIMS spectra peak-fitting and data processing was developed to calculate an accurate sulfur isotopic fractionation $\delta 34S_{V\text{-}CDT}$ on iron sulfide layers formed on iron surfaces, thus allowing to discriminate between abiotically *versus* biotically generated sulfides. This approach contributes to a better understanding of iron surface interactions with sulfur containing environmental species of abiotic or biotic origin.

Keywords: Biocorrosion, ToF-SIMS, Isotopic fractionation**,** Iron sulfides

1 Introduction

Biocorrosion or Microbially Influenced Corrosion (MIC) is a phenomenon defined as the involvement of microorganisms in the corrosion of metallic materials [1–4]. The metabolic activity of microorganisms can modify the chemistry of environment, especially the

metal/environment interface [5,6]. It is documented that microbial activity can lead to the modification of corrosion behavior and rates of the metallic materials.

MIC impacts several industrial sectors including the paper, nuclear, and petrochemical [7] industries, as well as public infrastructure. The cost of corrosion represents around 4% of the GNP (Gross National Product) for most countries [8–10] and, according to Flemming *et al.* [9], approximately 20% of the total cost is likely related to MIC. While numerous studies worlwide have focused on understanding MIC, the mechanisms are complex [11–15] and the phenomenon remains not well understood.

Several types of bacteria belonging to different genera and species such as iron-, sulfate-, or CO_2- reducing bacteria and iron-, sulfur- and manganese- oxidizing bacteria are implicated in MIC. Sulfate-Reducing Bacteria (SRB) are frequently the key-culprit in MIC [16]. SRB is a group composed of diverse anaerobic able to form sulfide following a dissimilatory sulphate-reduction [17–19]. The latter metabolic activity results in the formation of H_2S gas or HS^- ions, both of which are corrosive to metallic material and considered to be health and safety hazards [20,21]. The corrosion of iron in the presence of actively metabolizing SRB, can lead to the formation of different forms of sulfides compounds including mackinawite (tetragonal

50 FeS), pyrite (FeS_2), pyrrhotite ($Fe_{1-x}S$, where x = 0 to 0.2), troïlite (hexagonal FeS) and
51 greigite (Fe_3S_4) [22].
52 During the process of sulphate reduction, bacteria preferentially reduce light sulfur isotopes
53 rather than heavier isotopes. This phenomenon can be explained by thermodynamic
54 considerations, as dissociation of molecules differs between isotopes, the lightest making
55 weaker bonds compared to the heaviest [23]. Kinetic effects can also be involved, as
56 according to the so called “kinetic isotope effect”, bacteria can process lighter isotopes faster
57 than heavier ones [24].
58 Comparison of sulfur isotopic abundances in corrosion products is therefore a potentially
59 powerful tool for SRB – influenced corrosion diagnostics [25–27].
60 The isotopic ratio is defined as the ratio of the abundance of the two main isotopes. For
61 example, the sulfur isotopic ratio R34S is defined as:

$$R34S = \frac{\text{Abundance of } 34S}{\text{Abundance of } 32S} \qquad \textbf{Eq.(1)}$$

62 As shown by Thode *et al.* [28], the corrosion products resulting from MIC exhibit a different
63 isotopic ratio than those formed during abiotic corrosion. The isotopic ratio of corrosion
64 products formed in the absence of SRB, $R34S_{natural}$, is known to be 0.04519 [23,30]. It is
65 obtained from the sulfur natural abundances for the ^{32}S isotope and the ^{34}S isotope, which are

94.93% and 4.29% respectively [23,30]. In the case of MIC caused by SRB, due to bacterial preference for utilizing lighter isotopes, the isotopic ratio R34S is lower than that the "natural" one ($R34S_{natural}$). In this study, the difference in the sulfur isotopic ratio is aids to discriminate between the abiotic *versus* biotic corrosion process.

To make interlaboratory comparison [31], it is common to employ the notation of isotopic fractionation according to the equation below:

$$\delta 34S_{\,\mathrm{Standard}}(‰) = \left(\frac{\mathrm{R34S_{sample}}}{\mathrm{R34S_{Standard}}} - 1\right) \times 1000 \qquad \textbf{Eq.(2)}$$

The first standard used for sulfur isotopic composition was troïlite from the Canyon Diablo Troïlite (CDT) meteorite, which crashed in Arizona in 1891 [32–34]. However, Beaudoin *et al*. later proved isotopic inhomogeneity of the meteorite [35], making its use as reference material inadequate in order to compare data between laboratories.

In 1993, to avoid the problem of inhomogeneity and to make inter-comparisons, the International Atomic Energy Agency (IAEA) advisory group proposed a new reference material, called IAEA S-1 [36–38], which is an abiotic silver sulfide. The calibration of this new material *versus* the CDT scale was practically impossible, because of the inhomogeneity of the CDT. Thus, at the Consultants Meeting held in December 1993 in Vienna, it was proposed to adopt the IAEA S-1 isotopic fractionation value of $\delta 34S\,^{\mathrm{IAEA\,S-1}}_{\mathrm{V-CDT}}$= -0.3 ‰ *versus*

an hypothetical scale, called Vienna – Canyon Diablo Troïlite (V-CDT)[36,38]. It was recommended to normalize the isotopic sulfur composition data to the new V-CDT scale using the material reference IAEA S-1. The latter was artificially prepared from isotope-enriched elemental sulfur (^{32}S, ^{33}S and ^{34}S). The resultant species, $Ag_2{}^{32}S$, $Ag_2{}^{33}S$ and $Ag_2{}^{34}S$, prepared by the gravimetric methodology, formed an isotopic mixture of Ag_2S, which mimic the natural isotopic composition of studied materials [28]. The IAEA provided reference materials such as the IAEA S-1 to Ding *et al*. [36] and they measured the abundance ratio of the IAEA S-1, corresponding to $^{32}S/^{34}S$ = 22.6504. Because $\delta 34S_{V-CDT}^{IAEA\ S-1}$is -0.3 ‰, it was possible to calculate the V-CDT abundance ratio and the abundance ratio, which is 22.6436 (i.e. $R34S_{V\text{-}CDT}$ = 0.0441626). Under such conditions, the natural isotopic fractionation of sulfur can be calculated in the V-CDT scale and it is $\delta 34S_{V-CDT}^{natural}$ = 23,26 ‰.

In here presented investigation, all isotopic fractionations were calculated following the above listed equation **Eq.(2)** with respect to the V-CDT standard, using $R34S_{V\text{-}CDT}$ = 0.0441626.

Recent study [39] demonstrated that the ToF-SIMS can be used to identify the biotic and abiotic origins of iron sulfides. In this work [39], the sulfur isotopic ratio was directly calculated from the peak area in the ToF-SIMS spectra.

Here, to improve the accuracy of the method, as ^{32}S and $^{16}O_2$ give overlapping signals, and because ^{32}S and ^{34}S concentrations are directly correlated with peak areas in ToF-SIMS, a peak-fitting protocol is applied for fitting each peaks belonging to a specific mass range in order to have an accurate estimation of the proportion of the two isotopes, ^{32}S and ^{34}S, and thus, calculate the sulfur isotopic fractionation.

To establish the procedure, ToF-SIMS analysis of reliable reference materials is required. Two different reference materials corresponding to pure abiotic and biotic iron sulfides have been prepared and analyzed in the laboratory. The first part of this communication addresses the preparation of abiotic and biotic sulfides and the method used to obtain the ToF-SIMS data, while in the second part, the data processing is presented. Lastly, the peak-fitting method is applied to spectra of abiotic and biotic reference materials to precisely determine the sulfur isotopic fractionation $\delta 34S_{V\text{-}CDT}$ obtained from each reference material.

2 Materials and methods

2.1 *Abiotic sulfidation*

Pure iron samples (Goodfellow) were mechanically polished with diamond paste (ESCIL) down to ¼ µm, then sonicated in acetone (CARLO ERBA), ethanol (CARLO ERBA), and in

ultra-pure water, to obtain a clean and mirror polish finish. Samples were dried in a flow of compressed air.

The sulfidation was performed electrochemically using a Bio-Logic (SP) potentiostat connected to a conventional three electrode electrochemical cell, with the pure iron sample as working electrode, a saturated calomel electrode as reference and a platinum wire as counter electrode. The electrolyte was a 10^{-2} M Na_2S, $9H_2O$ (Sigma Aldrich) and 10^{-3} M NaOH (pH = 11) deaerated aqueous solution.

To reduce the oxide which naturally formed on the surface, a linear sweep voltammetry starting from the OCP down to a potential E = -1.25 V/SCE with a scan rate of 50 mV/s was first performed and the lower potential was maintained for 1 min. A potential step to -0.8 V/SCE (potential corresponding to the sulfide domain of the E-pH diagram) was applied and the potential was maintained during 50 min to produce iron sulfide on the surface.

Following electrochemical treatment, the sample, covered by a dark deposit, was dried using a flow of compressed air and transferred into the ToF-SIMS spectrometer, where it was immediately analysed.

2.2 *Biotic sulfidation*

To produce the biotic reference sample, the marine bacterium *Desulfovibrio alaskensis* (NCIMB 13491) was used. The organism has been isolated from a corroding steel installation [40]. Since SRB belong to an anaerobic group [41,42], the culture was grown in an anoxic medium composed of ($g.L^{-1}$ distilled water): NaCl, 20; $MgCl_2$, $6H_2O$, 3.0; $CaCl_2$, $2H_2O$, 0.15; NH_4Cl, 0.25; KH_2PO_4, 0.2; KCl, 0.5; sodium lactate 0.6; Na_2SO_4, 3.5; resazurine and trace element solution, the latter as reported by Zinkevich and Beech [41]. The pH was adjusted to 7.2 value by adding 0.1 M NaOH. Medium was deaerated with a N_2/CO_2 gas mixture for 2h and augmented with a vitamin solution [43]. Freshly prepared medium was sterilized through autoclaving at 121°C for 20 min, in order to avoid the presence of any micro-organism [41]. The inoculum that consisted of a two day old *Desulfovibrio alaskensis* (NCIMB 13491) culture, in exponential growth phase, was added to the sterile medium at 10% (v/v). The culture was grown at 37°C for 72h to ensure a high concentration of HS^- ions.

To expose the Fe sample to HS^- ions, and to exclude bacterial cells and sulfate to avoid contamination of the surface which could modify the sulfur isotopic fractionation, the bacteria were removed by collecting, after centrifugation (3 cycles, 15min each cycle at 17°C with 6500 rpm), the supernatant, and the sulfates were precipitated and filtered using 1 M

146 deaerated barium (Sigma Aldrich) chloride and sterile 0.22 µm filter. In this way, the obtained
147 aqueous medium contained only HS^- ions.
148 The sample was pure iron, mechanically polished with diamond paste down to ¼ µm to obtain
149 a mirror polish finish, and rinsed with acetone. All the preparation steps were carried out
150 aseptically, under anaerobic conditions. Finally, the sample was immersed in the medium
151 containing HS^- for 24h at the OCP and at room temperature. After immersion, the specimen
152 was rinsed with UP water and stored in a sterile glass tube filled with N_2 gas to prevent
153 surface modification and contamination.
154
155 **2.3** *ToF-SIMS measurements*
156 ToF-SIMS is a surface sensitive technique that allows us to analyse elements, isotopes or
157 molecules which are present on a surface. A major feature of this spectrometry is its very high
158 sensitivity with a detection limit around ppb and the possibility to detect isotopes.
159 As previously discussed by Seyeux and Marcus [39], the ToF-SIMS is fully appropriate for
160 the study of the abiotic or biotic origin of sulfides formed on surfaces.
161 To reach both high mass resolution (m/Δm around 7 000) and high lateral resolution (around
162 200 nm), the spectrometer was used in the BA-IMAGE (Burst-Alignment Image) mode where

each primary pulse was split in 4 pulses (burst mode). A high lateral resolution mode has been used in order to be able to apply the method to complex samples that can be non-homogeneous, with both Fe sulfides and Fe oxides present at the surface. A low primary current is necessary to avoid the saturation of the $^{32}S^-$ signal that would lead to an underestimation of the sulfur isotopic fractionation $\delta 34S_{V\text{-}CDT}$.

ToF-SIMS analyses were performed using a ToF-SIMS V spectrometer (IonToF – Munster Germany). The spectrometer was operated at a pressure of 10^{-9} mbar. A pulsed 25 keV Bi^+ primary ion source was used for analysis, delivering 0.03 pA over a 100 x 100 µm² area. 2D spectra of negatively charged ions were recorded. Each sample was analysed two times on two randomly selected areas. Data acquisition and post-processing were carried out using Surface Lab 6.7 software.

Before each measurement, the extreme surface was sputtered for a period of 10s using a Cs^+ ion sputter gun to remove any surface contamination. The sputter gun used delivered 120 nA over a 500 x 500 µm² area.

As previously shown by Grousset [44], it is necessary to reach a minimum of fluence around 10^{13} ions/cm² to stabilize the sulfur isotopic fractionation. Thus, only the data from 10^{13}

ions/cm² and up were used to calculate the sulfur isotopic fractionation. Here, the spectra were acquired during sufficiently long time to reach a fluence of, at least, 3.10^{13} ions/cm². To improve the accuracy of the determination of the sulfur isotopic fractionation, from ^{32}S and ^{34}S peak areas, all spectra were fitted using the method described in §2.4.

2.4 *Peak-fitting method using CasaXPS software*

ToF-SIMS peak-fitting has been already done in different studies. In the work of Cliff *et al.* [45], a peak-fitting algorithm was developed to remove interferences of Al^- and $^{13}C^{14}N^-$ from $^{12}C^{15}N^-$, because in this work low mass resolution was used.

More recently, the fit of ToF-SIMS spectra using CasaXPS software was done in the work of Abel *et al.* [46]. The aim of their peak-fitting method was to correlate the peak shape, including both full width at half-maximum FWHM and asymmetry, to surface information such as roughness and oxide thickness. They use of a mathematic function combining Lorentzian (70%) and Gaussian (30%) with the addition of an asymmetry factor, allowed them to establish a link between the asymmetry factor and the FWHM with the oxide thickness and the roughness. The same methodology was used by Shimizu *et al*. [47] and Dou *et al*. [48].

196 Here, CasaXPS software was used for data processing. This software is commonly employed
197 for the processing of XPS and Auger data. Recently, a module for processing ToF-SIMS data
198 has been added [49]**.** One of the main differences between XPS and ToF-SIMS data
199 processing, in terms of peak-fitting, is the asymmetry of the peak side and the background.
200 While the peak shape and the background are directly associated to physical phenomena in
201 XPS (these are correlated to an electronic emission process) [50–52], the physical parameters
202 related to the peak shape have not been yet clearly identified for ToF-SIMS measurements. In
203 our work, the CasaXPS software was used to determine the functional of the instrumental
204 response, allowing us to fit the peaks, without considering any specific physical factor.
205 In this investigation, the peak-fitting method was used to process data, in which there are
206 mass interferences (Table 1) in the $^{32}S^-$ and $^{34}S^-$ regions, in order to determine an accurate
207 sulfur isotopic fractionation.

	Element (amu)			
Mass range from 31.95 to 32.02	**^{32}S** **(31.972)**	$^{31}P^{1}H$ (31.982)	$^{16}O_2$ (31.990)	
Mass range from 33.95 to 34.02	**^{34}S**	$^{33}S^{1}H$	$^{1}H_2\,^{32}S$	$^{18}O^{16}O$

	(33.968)	(33.979)	(33.988)	(33.994)

Table 1: Possible mass interferences for each mass range ($^{32}S^-$ and $^{34}S^-$)

While processing our ToF-SIMS data, no background was used and the peak-fitting was done with a LA line shape (Lorentzian Asymmetric). First, the symmetric Lorentzian line shape L(f,m/z) is given by:

$$L(x: f, m/z) = \frac{1}{1 + 4 \times (\frac{x - m/z}{f})^2} \qquad \text{Eq.(3)}$$

The asymmetric Lorentzian line shape LA(α,β) is:

$$LA(\alpha, \beta) = \begin{cases} [L(x: f, m/z)]^{\alpha} & x \leq m/z \\ [L(x: f, m/z)]^{\beta} & x > m/z \end{cases} \qquad \text{Eq.(4)}$$

Where f is the full width at half-maximum (FWHM), m/z is the mass/charge ratio, and α, β are the parameters to determine.

The LA(α, β) line shape was operated with the addition of a Gaussian convolution, written LA(α, β, *n*) where *n* (between 0 and 499) is a parameter controlling the width of a Gaussian convolution applied to the functional form.

For defining the α, β and *n* peak-fitting parameters, the $^{37}Cl^-$ peak was chosen as reference peak, because it is close in mass to $^{32}S^-$ and $^{34}S^-$, and not affected by overlapping with any

other signals. With the $^{37}Cl^-$ peak, it is possible to determine the functional of the instrumental response for each analysis.

As shown on the Figure 1, the procedure was first to fit the ^{37}Cl peak with the LA(α, β, *n*) line shape.

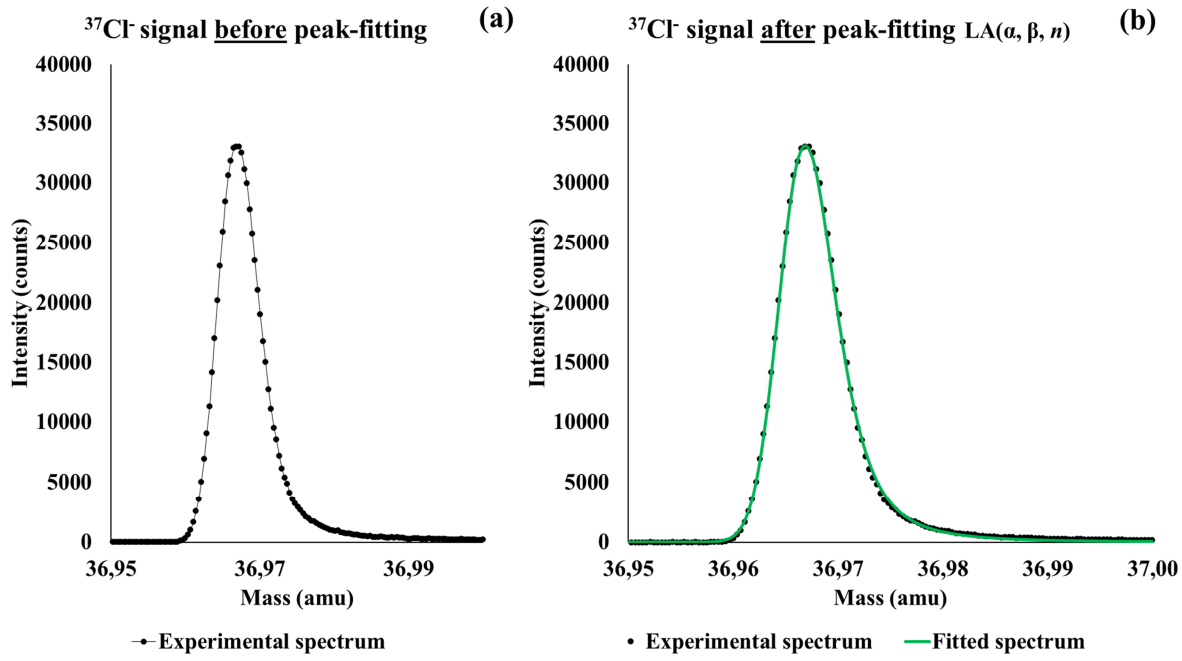

Figure 1: Peak-fitting of the $^{37}Cl^-$ signal in order to determine the best α, β and *n* parameters: **(a)** before and **(b)** after peak-fitting

The obtained α, β and *n* parameters are then directly used to fit both ^{32}S and ^{34}S mass ranges using the LA line shape (it is assumed that the peak shapes remain the same in the investigated mass spectrum). Thus, the best fit of the experimental data with all possible species taken into account (see Table 1) is obtained.

This fitting methodology allows us to determine the percentage of each element present in both ^{32}S and ^{34}S mass ranges. In this way, precise proportions of $^{32}S^-$ and $^{34}S^-$ are determined and used for the calculation of the sulfur isotopic fractionation $\delta 34S_{V\text{-}CDT}$.

Each sample was analyzed two times using different areas. On each area, since a primary beam fluence over 3.10^{13} ions/cm^2 is needed, several primary ion pulses are given to the surface. Thus, as a mass spectrum is associated to each individual primary pulse, several spectra were obtained (around 5000 mass spectra are recorded on each analyzed areas of the sample). For each sample (abiotic and biotic iron sulfides), the mean sulfur isotopic fractionation $\delta 34S_{V\text{-}CDT}$ corresponds to the maximum of the Gaussian curve used to fit the statistical distribution of $\delta 34S_{V\text{-}CDT,}$ calculated from all mass spectra for the 2 areas on each sample (i.e. around 10000 mass spectra per sample).

The uncertainty on the mean sulfur isotopic fractionation value, as well as the standard deviation, are also given by the fit of the statistical distribution of $\delta 34S_{V\text{-}CDT}$.

3 Results and discussions

Figure 2.a, Figure 3.a, Figure 4.a and Figure 5.a depict the raw ToF-SIMS data obtained on abiotic and biotic iron sulfide samples in the ^{32}S and ^{34}S mass ranges (between 31.95 and 32.02 amu, and between 33.95 and 34.02 amu, respectively). These figures directly evidence

248 the mass interferences in the ^{32}S and ^{34}S regions on both biotically and abiotically generated
249 sulfides. The presence of $^{16}O_2^-$ signal, resulting from the sample preparation method, i.e.
250 exposure in aqueous environment, is overlapping with the $^{32}S^-$ signal and causes an
251 overestimation of the ^{32}S intensity. Consequently, uncertainty in the calculation of the sulfur
252 isotopic fractionation $\delta 34S_{V\text{-}CDT}$ can make difficult to distinguish abiotic and biotic processes,
253 therefore the origin of iron sulfidation. Careful processing of the experimental data through a
254 peak-fitting procedure, to extract the most accurate proportion of $^{32}S^-$ and $^{34}S^-$ and to calculate
255 a relevant sulfur isotopic fractionation $\delta 34S_{V\text{-}CDT}$, is thus of paramount importance.
256 The peak-fitting was carried out with the methodology described previously in §2.4. First, the
257 α, β and *n* parameters are determined based on the position of the $^{37}Cl^-$ peak. Then, the LA
258 line shape and these parameters are applied on the possible mass interferences. Since no ^{31}P
259 isotope is detected in the mass spectra, it is assumed that the $^{31}P^1H$ component is not present
260 in abiotic and biotic samples in the ^{32}S mass range. Thus only $^{32}S^-$ and $^{16}O_2^-$ are considered
261 (between 31.95 and 32.02 amu). The fitted spectrum (in **green**) is the sum of both considered
262 components, i.e. $^{32}S^-$ (in **orange**) and $^{16}O_2^-$ (in **blue**). The experimental peak (in **black**) is well
263 fitted applying this model (Figure 2.b, Figure 4.b). After peak fitting we checked that the
264 residual was always < 1% of the peak.

A similar procedure was applied for the $^{34}S^-$ mass range. The results are presented in Figure 3.b and Figure 5.b (between 33.95 and 34.02 amu). In this latter mass range, four species must be considered: $^{34}S^-$ (in **purple**), $^{33}S^1H^-$ (in **pink**), $H_2{}^{32}S^-$ (in **turquoise**) and $^{18}O^{16}O^-$ (in **grey**). The presence of $^{33}S^1H^-$ and $^{18}O^{16}O^-$ species is confirmed by the presence of $^{32}S^1H^-$ and $^{16}O_2^-$ species. Again, the fitted spectrum (in **green**) fits very well the experimental spectrum. After peak fitting we checked that the residual was always < 1% of the peak.

The fit parameters are LA(9,1.45,80) for abiotically generated iron sulfide and LA(9,1.55,80) for the biotic iron sulfide samples.

It is important to note that during ToF-SIMS data processing, a slight difference in the β parameter value is observed as function of the sample procedure (abiotic or biotic). The measurements have been performed on different days, hence, the slight variation in the value of β parameter could be due to fluctuation in the fine settings of ToF-SIMS instrument. Moreover, as reported by M.L Abel *et al.*[46], the oxide thickness may modify the peak asymmetry. Indeed, sulfide thickness differences between the samples could explain the differences in the value of β parameter used for peak-fitting. Finally, the sulfide chemical composition on the value of β parameter cannot be excluded.

To minimize the uncertainty due to topographic, composition and thickness variations, it was deemed more appropriate to fit the $^{37}Cl^-$ peak and to determine the three α, β and *n* parameters for each mass spectrum. The proportion of ^{32}S and ^{34}S peaks were then estimated with higher accuracy, and the sulfur isotopic fractionation $\delta 34S_{V\text{-}CDT}$ was recalculated.

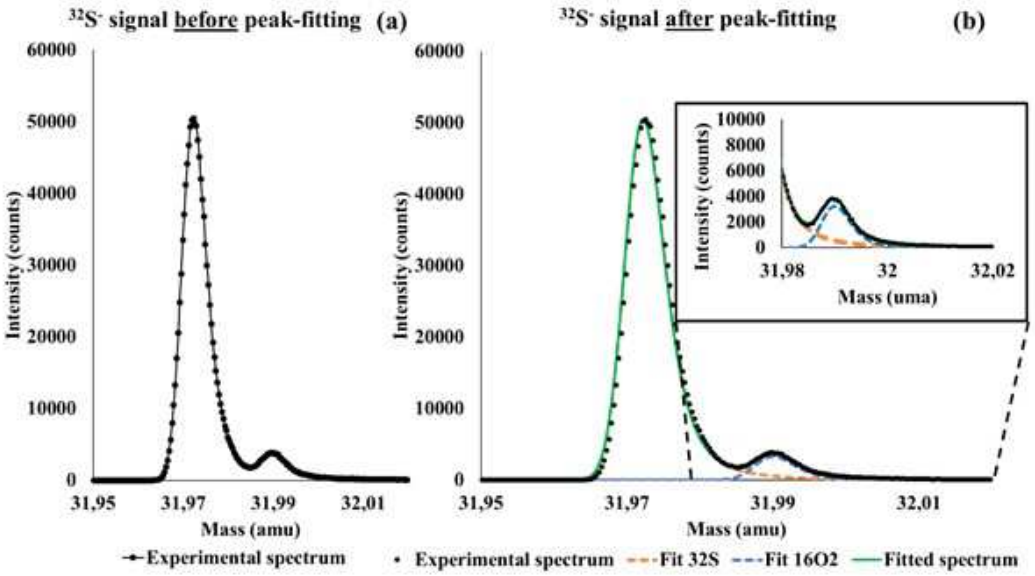

Figure 2:The $^{32}S^-$ signals before **(a)** and after **(b)** peak-fitting on abiotic iron sulfide formed by electrochemical treatment in 10^{-2} M Na_2S, $9H_2O$ and 10^{-3} M NaOH (pH = 11) deaerated aqueous solution.

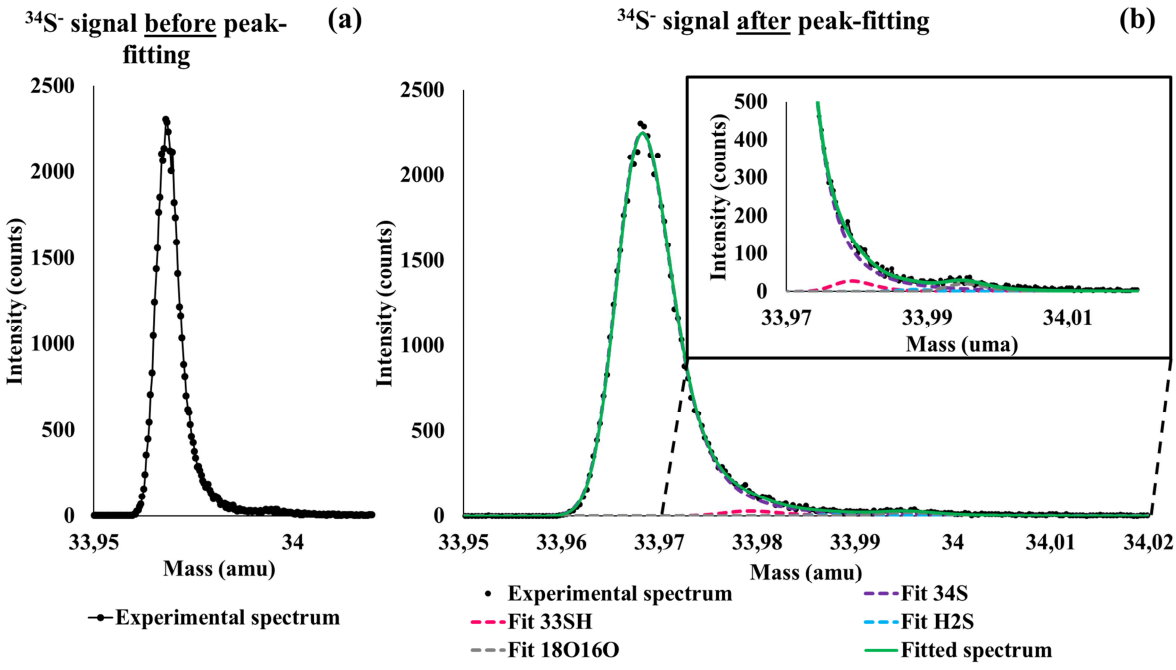

289

290 Figure 3: The $^{34}S^-$ signals before **(a)** and after **(b)** peak-fitting on abiotic iron sulfide formed

291 by electrochemical treatment in 10^{-2} M Na_2S, $9H_2O$ and 10^{-3} M NaOH (pH = 11) deaerated

292 aqueous solution.

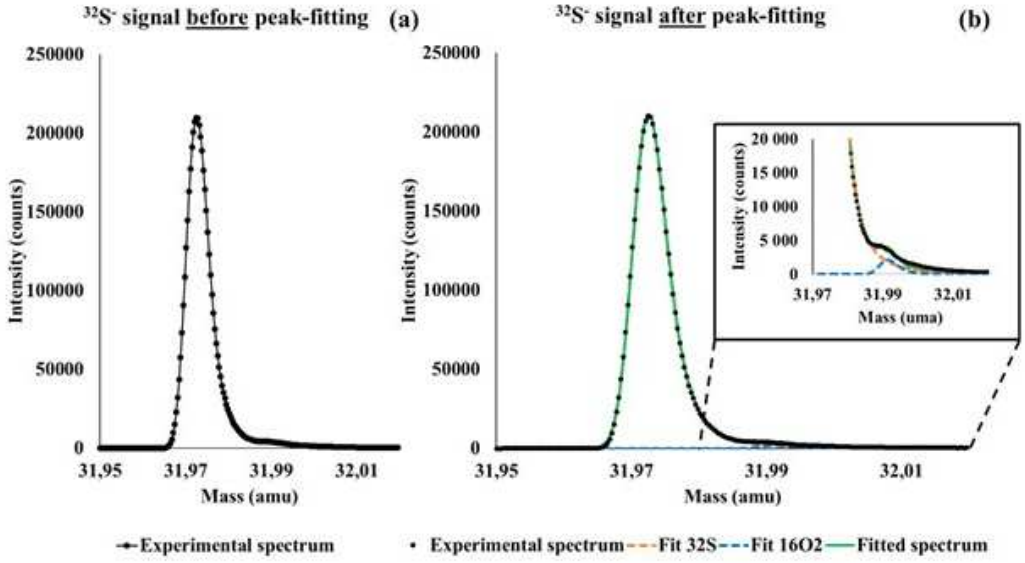

293

294 Figure 4:The $^{32}S^-$ signals before **(a)** and after **(b)** peak-fitting on biotic iron sulfide formed in

295 solution containing HS^- ions generated by metabolic activity of SRB.

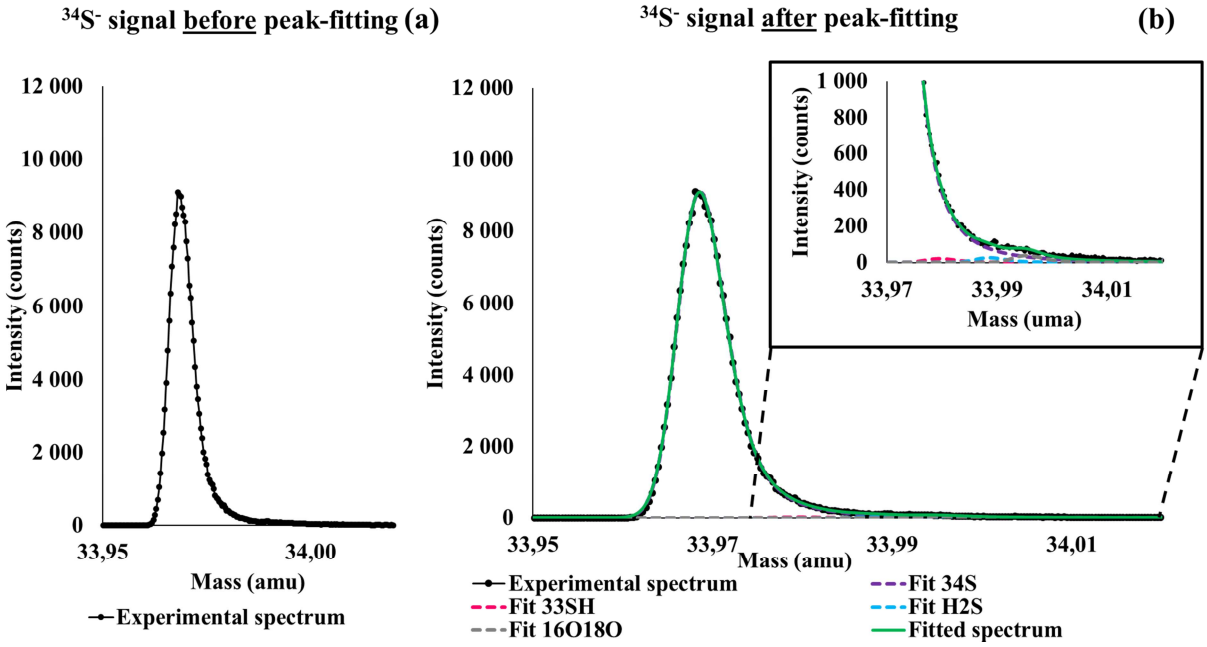

296

297 Figure 5: The $^{34}S^-$ signals before (a) and after (b) peak-fitting on biotic iron sulfide formed in

298 solution containing HS^- ions generated by metabolic activity of SRB.

299 Figure 6 shows the mean sulfur isotopic fractionation $\delta 34S_{V\text{-}CDT}$, from abiotic and biotic

300 samples, determined from the statistical treatment of the distribution of $\delta 34S_{V\text{-}CDT}$ calculated

301 from peak fitted mass spectra, as described in details above.

302 In figure 6, the zero corresponds to the V-CDT standard value [36] and the natural sulfur

303 isotopic fractionation is calculated with the natural abundances of sulfur (given in tables

304 [23,30]) i.e. $\delta 34S_{V\text{-}CDT} = 23.26$ ‰, as previously explained in §1.

In Grousset's investigation [44], the authors analysed $BaSO_4$, formed from Na_2SO_4 present in the growing medium, with IRMS (Isotopic Ratio Mass Spectrometry) and they reported an sulfur isotopic fractionation $\delta 34S_{V\text{-}CDT}$ = **27.88 (± 1.32) ‰**, which is similar to the natural sulfur isotopic fractionation.

In here presented work, Na_2SO_4 (that was used as a source of iron sulfide) comes from the same supplier than the one used in Grousset's work. For safety reasons, Na_2S, $9H_2O$ could not be analysed with IRMS. Thus, it is assumed that Na_2S, $9H_2O$ and Na_2SO_4 have the same sulfur isotopic fractionation and that it is close to the natural value of 23.26 ‰.

Figure 7.a and.b show the distribution of the sulfur isotopic fractionation $\delta 34S_{V\text{-}CDT}$ (calculated from corrected intensities of ^{32}S and ^{34}S according to the peak-fitting procedure) of the abiotic and biotic substrates, respectively. The statistical distribution of $\delta 34S_{V\text{-}CDT}$ is very well fitted by a Gaussian law, allowing us to determine the mean sulfur isotopic fractionation $\delta 34S_{V\text{-}CDT}$, and the uncertainty of the mean value for the abiotic and biotic samples. For the abiotic iron sulfide, the mean sulfur isotopic fractionation value is **-0.23 (± 0.54) ‰** while for biotic iron sulfide, the value is **-13.69 (± 0.45) ‰**.

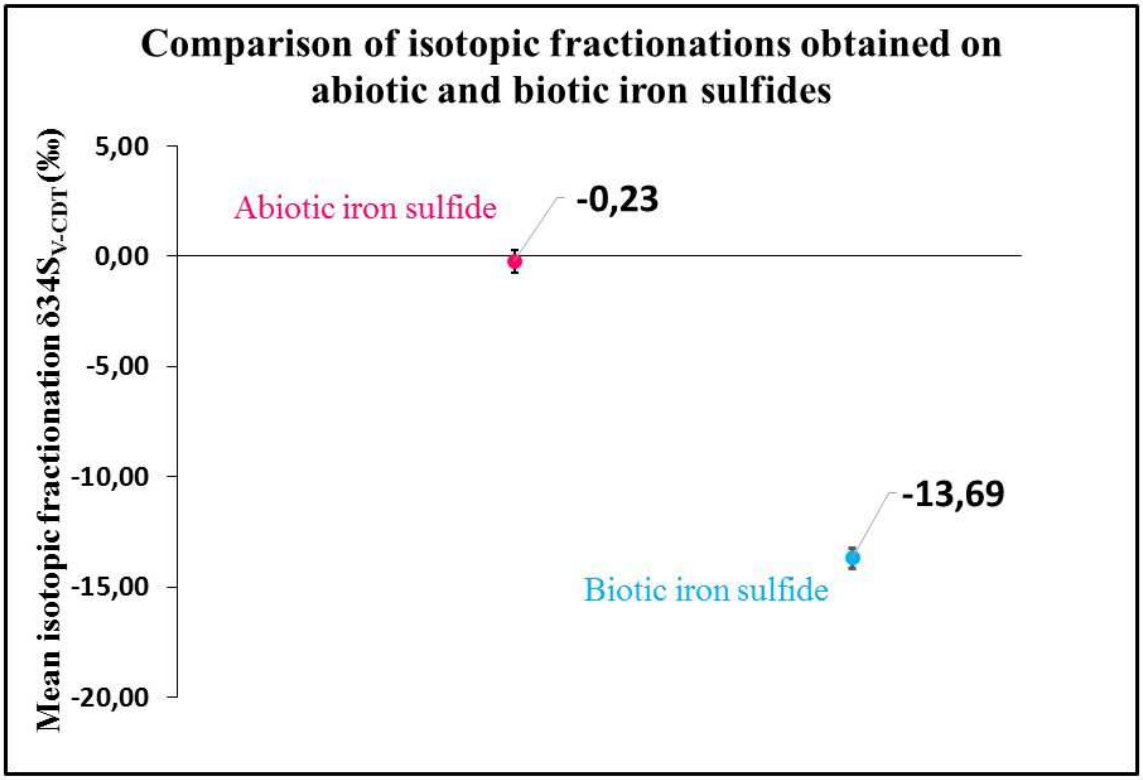

320

321 Figure 6: Mean values of sulfur isotopic fractionations obtained in iron sulfides produced in

322 aqueous solutions at room temperature by abiotic (electrochemical preparation) and biotic

323 (bacterial origin) processes.

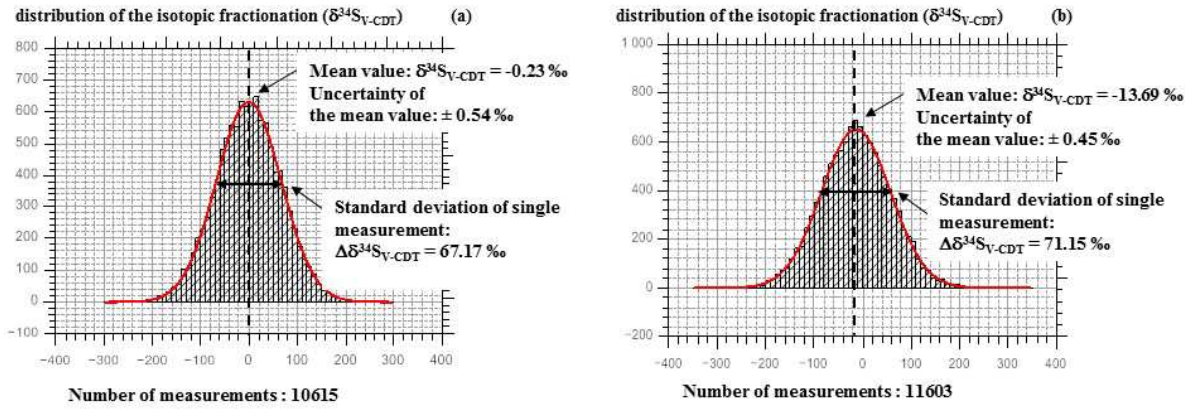

324

Figure 7: Statistical distribution of $\delta 34S_{V\text{-}CDT}$ calculated from mass spectra obtained on the 2 analyzed areas of (a) the abiotic iron sulfide and (b) the biotic iron sulfide showing the fit by a Gaussian law. The results from the fitting, i.e. mean sulfur isotopic fractionation ($\delta 34S_{V\text{-}CDT}$), uncertainty of the mean value, and standard deviation of single values ($\Delta\delta 34S_{V\text{-}CDT}$) are indicated.

It is apparent that the abiotic and biotic sulfur isotopic fractionation mean values are significantly different (-0.23 *vs* -13.69, respectively). Moreover the low uncertainty on these values makes clearly possible the distinction between the abiotic and biotic iron sulfides formed in aqueous conditions at room temperature. Nevertheless, it is important to point out that the sulfur isotopic fractionation standard deviation on simgle measurements ($\Delta\delta 34S_{V\text{-}CDT}$) is large (67.17 ‰ and 71.15 ‰ for abiotic and biotic reference samples, respectively). This is related to the ToF-SIMS spectrometer and the analysis conditions used to record the data. Thus, a sufficient large number of measurements must be collected on each sample to determine accurately the mean sulfur isotopic fractionation value and the uncertainty on this mean value. In our work, the mean sulfur isotopic fractionation being the result of at least 10000 mass spectra, the statistical distribution of the sulfur isotopic fractionation is well fitted

342 by a Gaussian law, making the determination of the mean sulfur isotopic fractionation
343 possible with a low uncertainty.
344 This investigation has demonstrated the capability of ToF-SIMS to distinguish the abiotic or
345 biotic origin of iron sulfides formed in aqueous conditions at room temperature, if a sufficient
346 number of data points is recorded and peak fitting treatment of the mass spectra used to
347 remove the possible mass interferences in the $^{32}S^-$ and $^{34}S^-$ mass regions.
348 It is also worthwhile noting that the sulfur isotopic fractionation calculated for the abiotic
349 sample is close to the that of standard V-CDT value ($\delta 34S_{V\text{-}CDT}$ = 0 ‰). This observation is
350 not surprising considering the chemical environment for the formation of the V-CDT
351 standard. The standard value is in agreement with the type of sulfur isotopic fractionation
352 which occurs during an abiotic sulfide-influenced corrosion process.
353 The more negative sulfur isotopic fractionation (-13.69 ‰) obtained from the biotic sample
354 indicates that the sulfide is enriched in ^{32}S, as predicted for biotic corrosion [53].
355 The sulfur isotopic fractionation obtained using abiotic sample (-0.23 ‰) is clearly below the
356 natural sulfur isotopic fractionation ($\delta 34S_{V\text{-}CDT}$ = 23.26 ‰ in average).
357 It has been shown by Harrison and Thode that there was isotopic fractionation during the
358 chemical reduction of sulfate to sulfide, including several chemical reaction steps [54].

359 Thode *et al.* [28] analysed sulfur dioxide gas produced by the combustion of iron sulfide
360 under a flow of O_2 gas and did not observe any isotopic fractionation.
361 Here, an isotopic fractionation is recorded following the abiotic reaction. As already
362 explained above, it is difficult to predict the chemical reaction, regardless whether it is biotic
363 or abiotic reaction which would lead to an isotopic fractionation. Thus, in our work, an effect
364 of the abiotic reaction on the isotopic fractionation cannot be excluded.
365 However, in that case, the difference between abiotic and biotic isotopic fractionation would
366 be even larger, making easier the identification of the biotic process.
367 The variability could originate from the surface finish as explained by Kita *et al.* [55,56]. The
368 roughness or scratches on the surface can influence the variability of the isotopic
369 fractionation. The sample topography can create a deformation of the electrostatic field
370 applied to the sample surface. This deformation could modify the trajectory of secondary ions
371 and result in fractionation of isotopes having different masses.
372 In summary, using ToF-SIMS as an analytical technique, combining the analysis with data
373 processing using CasaXPS software and a proper statistical analysis of the data allows to
374 distinguish between the origins of the two iron sulfides. To apply this approach to the analysis
375 of other samples, on which the iron sulfide layer is heterogeneous in thickness (e.g. localized

sulfides forming islands on the surface), local sulfur isotopic fractionation measurement will require both high lateral and high mass resolutions.

4 Conclusions

Two kinds of iron sulfide layers, abiotic and biotic, have been prepared on iron surfaces. The abiotic iron sulfide layer was electrochemically obtained in an aqueous solution of Na_2S (10 mM) on pure iron. The biotic iron sulfide layer was obtained by immersion of an iron sample in a solution containing HS^- produced by bacteria (SRB). ToF-SIMS with high mass resolution and high lateral resolution was used to analyse biotically and abiotically formed iron sulfides on iron surfaces. The data were processed using CasaXPS software to fit the $^{32}S^-$ mass region and subtract the $^{16}O_2^-$ contribution, and the $^{34}S^-$ mass region and subtract the $^{33}S^1H^-$ and $H_2{}^{32}S^-$ contributions.

The sulfur isotopic fractionation values that were calculated from the areas of $^{32}S^-$ and $^{34}S^-$ peaks, revealed significant statistical difference between abiotic and biotic sulfides, namely **-0.23 (± 0.54) ‰** for the abiotic iron sulfide and to **-13.69 (± 0.45) ‰** for the biotically generated iron sulfide.

The reported data demonstrate that employing ToF-SIMS allows us to distinguish between abiotic and biotic iron sulfide layers, and that ToF-SIMS measurements with high mass

resolution correlated with an appropriate data processing (peak-fitting) procedure of the ^{32}S and ^{34}S regions and the acquisition of a sufficient number of mass spectra on a given substrate would allow the determination of a precise sulfur isotopic fractionation and would facilitate identification of the origin of sulfide-rich corrosion products on iron or steel surfaces. It is proposed that using the high lateral resolution mode of ToF-SIMS (~100-200 nm), the method is suitable for investigating the origin of corrosion in sulfidogenic environments, including surfaces on which sulfide corrosion products are unevenly distributed. It is proposed that ToF-SIMS platform can serve as a tool for investigating bacterial contribution to sulfide-driven corrosion, thus allowing a better understanding of biocorrosion, and an improvement of the corrosion protection strategy.

Acknowledgements

We thank Neal Fairley for his help in using CasaXPS software.

References

[1] B. Little, P. Wagner, Myths related to microbiologically influenced corrosion, Mater. Perform. 36 (1997).

[2] I. Beech, A. Bergel, A. Mollica, H.-C. Flemming, V. Scotto, W. Sand, Simple Methods for the Investigation of the Role of Biofilms in Corrosion, European Federation of Corrosion, 2000.

[3] B.J. Little, T.L. Gerke, R.I. Ray, J.S. Lee, The Mineralogy of Microbiologically Influenced Corrosion, in: Miner. Scales Depos., Elsevier, 2015: pp. 107–122.

[4] W.A. Hamilton, Sulphate-Reducing Bacteria and Anaerobic Corrosion, Annu. Rev. Microbiol. 39 (1985) 195–217.

[5] B.J. Little, J.S. Lee, Microbiologically influenced corrosion, Wiley-Interscience, Hoboken, N.J, 2007.

[6] D. Thierry, W. Sand, Microbially influenced corrosion, in: Corros. Mech. Theory Pract. Third Ed., CRC Press, Edited by Philippe Marcus, 2011: pp. 737–776.

[7] S.C. Dexter, C. Hahin, R.M. Kain, A.I. Asphahani, W.L. Silence, Localized corrosion, ASM Handb. 13 (1987) 104–122.

[8] R. Javaherdashti, How corrosion affects industry and life, Anti-Corros. Methods Mater. 47 (2000) 30–34.

[9] E. Heitz, H.-C. Flemming, W. Sand, Microbially influenced corrosion of materials: scientific and engineering aspects, Springer-Verlag, 1996.

[10] I.B. Beech, C.C. Gaylarde, Recent advances in the study of biocorrosion: an overview, Rev. Microbiol. 30 (1999) 117–190.

[11] H.A. Videla, L.K. Herrera, Understanding microbial inhibition of corrosion. A comprehensive overview, Int. Biodeterior. Biodegrad. 63 (2009) 896–900.

[12] I.B. Beech, Biocorrosion: Role of Sulfate Reducing Bacteria, in: G. Bitton (Ed.), Encycl. Environ. Microbiol., John Wiley & Sons, Inc., Hoboken, NJ, USA, 2003.

[13] N.O. San, H. Nazır, G. Dönmez, Microbially influenced corrosion and inhibition of nickel–zinc and nickel–copper coatings by Pseudomonas aeruginosa, Corros. Sci. 79 (2014) 177–183.

[14] B.E. Torres Bautista, M.L. Carvalho, A. Seyeux, S. Zanna, P. Cristiani, B. Tribollet, P. Marcus, I. Frateur, Effect of protein adsorption on the corrosion behavior of 70Cu–30Ni alloy in artificial seawater, Bioelectrochemistry. 97 (2014) 34–42.

[15] B.E. Torres Bautista, A.J. Wikieł, I. Datsenko, M. Vera, W. Sand, A. Seyeux, S. Zanna, I. Frateur, P. Marcus, Influence of extracellular polymeric substances (EPS) from Pseudomonas NCIMB 2021 on the corrosion behaviour of 70Cu–30Ni alloy in seawater, J. Electroanal. Chem. 737 (2015) 184–197.

[16] P. Angell, K. Urbanic, Sulphate-reducing bacterial activity as a parameter to predict localized corrosion of stainless alloys, Corros. Sci. 42 (2000) 897–912.

[17] B. Brunner, S.M. Bernasconi, A revised isotope fractionation model for dissimilatory sulfate reduction in sulfate reducing bacteria, Geochim. Cosmochim. Acta. 69 (2005) 4759–4771.

[18] A. Marietou, H. Røy, B.B. Jørgensen, K.U. Kjeldsen, Sulfate Transporters in Dissimilatory Sulfate Reducing Microorganisms: A Comparative Genomics Analysis, Front. Microbiol. 9 (2018).

[19] R. Rabus, T.A. Hansen, F. Widdel, Dissimilatory Sulfate- and Sulfur-Reducing Prokaryotes, in: E. Rosenberg, E.F. DeLong, S. Lory, E. Stackebrandt, F. Thompson (Eds.), The Prokaryotes, Springer Berlin Heidelberg, Berlin, Heidelberg, 2013: pp. 309–404.

[20] N. Pfennig, F. Widdel, H.G. Trüper, The Dissimilatory Sulfate-Reducing Bacteria, in: M.P. Starr, H. Stolp, H.G. Trüper, A. Balows, H.G. Schlegel (Eds.), The Prokaryotes, Springer Berlin Heidelberg, Berlin, Heidelberg, 1981: pp. 926–940.

[21] J.R. Postgate, The sulphate-reducing bacteria, CUP Archive, 1979.

[22] D. Rickard, G.W. Luther, Chemistry of Iron Sulfides, Chem. Rev. 107 (2007) 514–562.

[23] J. Hoefs, Stable isotope geochemistry, Sixth edition, Springer, Berlin, 2009, p.5.

[24] A.G. Harrison, H.G. Thode, Mechanism of the bacterial reduction of sulphate from isotope fractionation studies, Trans. Faraday Soc. 54 (1958) 84.

[25] H.C. Urey, The thermodynamic properties of isotopic substances, J. Chem. Soc. Resumed. (1947) 562–581.

[26] K.L. Cook, The Relative Abundance of the Isotopes of Potassium in Pacific Kelps and in Rocks of Different Geologic Age, Phys. Rev. 64 (1943) 278–293.

[27] H.G. Thode, Variations in abundances of isotopes in nature., Res. J. Sci. Its Appl. 2 (1949) 154.

[28] H.G. Thode, J. Macnamara, C.B. Collins, Natural variations in the isotopic content of sulphur and their significance, Can. J. Res. 27b (1949) 361–373.

[29] H.. Thode, Sulphur Isotopes in Nature and the Environment: An Overview, in: Stable Isot. Assess. Nat. Anthropog. Sulphur Environ., H.R. Krouse and V.A. Grinenko, H.R. Krouse and V.A. Grinenko, 1991.

[30] K.J.R. Rosman, P.D.P. Taylor, Isotopic compositions of the elements 1997 (Technical Report), Pure Appl. Chem. 70 (1998) 217–235.

[31] T.B. Coplen, Guidelines and recommended terms for expression of stable-isotope-ratio and gas-ratio measurement results: Guidelines and recommended terms for expressing stable isotope results, Rapid Commun. Mass Spectrom. 25 (2011) 2538–2560.

[32] J. Macnamara, H.G. Thode, Comparison of the Isotopic Constitution of Terrestrial and Meteoritic Sulfur, Phys. Rev. 78 (1950) 307–308.

[33] M.L. Jensen, N. Nakai, Sulfur isotope meteorite standards, results and recommendations, Biogeochem. Sulfur Isot. 35 (1962).

[34] V.F. Buchwald, Handbook of iron meteorites, Theier Hist. Distrib. (1975).

[35] G. Beaudoin, B.E. Taylor, D. Rumble, M. Thiemens, Variations in the sulfur isotope composition of troilite from the Cañon Diablo iron meteorite, Geochim. Cosmochim. Acta. 58 (1994) 4253–4255.

[36] T. Ding, S. Valkiers, H. Kipphardt, P. De Bi?vre, P.D.P. Taylor, R. Gonfiantini, R. Krouse, Calibrated sulfur isotope abundance ratios of three IAEA sulfur isotope reference materials and V-CDT with a reassessment of the atomic weight of sulfur, Geochim. Cosmochim. Acta. 65 (2001) 2433–2437.

[37] T. Ding, R. Bai, Y. Li, D. Wan, X. Zou, Q. Zhang, Determination of the absolute32S/34S ratio of IAEA-S-1 reference material and V-CDT sulfur isotope standard, Sci. China Ser. Earth Sci. 42 (1999) 45–51.

[38] Robinson, Reference and intercomparison materials for stable isotopes of light elements, (1993) 13–30.

[39] A. Seyeux, P. Marcus, Analysis of the chemical or bacterial origin of iron sulfides on steel by time of flight secondary ion mass spectrometry (ToF-SIMS), Corros. Sci. 112 (2016) 728–733.

[40] M.J. Feio, Desulfovibrio alaskensis sp. nov., a sulphate-reducing bacterium from a soured oil reservoir, Int. J. Syst. Evol. Microbiol. 54 (2004) 1747–1752.

[41] V. Zinkevich, I.B. Beech, Screening of sulfate-reducing bacteria in colonoscopy samples from healthy and colitic human gut mucosa, FEMS Microbiol. Ecol. 34 (2000) 147–155.

[42] H.F. Castro, N.H. Williams, A. Ogram, Phylogeny of sulfate-reducing bacteria(1), FEMS Microbiol. Ecol. 31 (2000) 1–9.

[43] W.E. Balch, G.E. Fox, L.J. Magrum, C.R. Woese, R.S. Wolfe, Methanogens: Reevaluation of a Unique Biological Group, Microbiol.Rev. 43 (1979) 37.

[44] S. Grousset, Détermination de la composition isotopique du soufre pour l'étude de l'origine, biotique ou abiotique, des sulfures de fer en corrosion anoxique, Université Pierre et Marie Curie (Paris 6), 2016.

[45] J.B. Cliff, D.J. Gaspar, P.J. Bottomley, D.D. Myrold, Peak fitting to resolve CN^- isotope ratios in biological and environmental samples using TOF-SIMS, Appl. Surf. Sci. 231–232 (2004) 912–916.

[46] M.L. Abel, K. Shimizu, M. Holliman, J.F. Watts, Peak-fitting of high resolution ToF-SIMS spectra: a preliminary study, Surf. Interface Anal. 41 (2009) 265–268.

[47] K. Shimizu, C. Phanopoulos, R. Loenders, M.-L. Abel, J.F. Watts, The characterization of the interfacial interaction between polymeric methylene diphenyl diisocyanate and aluminum: a ToF□SIMS and XPS study, Surf. Interface Anal. 42 (2010) 1432–1444.
[48] B. Dou, L.M. Wheeler, J.A. Christians, D.T. Moore, S.P. Harvey, J.J. Berry, F.S. Barnes, S.E. Shaheen, M.F. van Hest, Degradation of highly alloyed metal halide perovskite precursor inks: mechanism and storage solutions, ACS Energy Lett. 3 (2018) 979–985.
[49] N. Fairley, CasaXPS software version 2.3. 17, Casa Softw. Ltd U. K. (2014).
[50] S. Doniach, S. Doniach and M. Šunjić, J. Phys. C 3, 287 (1970)., J Phys C. 3 (1970) 286.
[51] J.W. Gadzuk, M. Šunjić, Excitation energy dependence of core-level x-ray-photoemission-spectra line shapes in metals, Phys. Rev. B. 12 (1975) 524–530.
[52] E. Sacher, Asymmetries in Transition Metal XPS Spectra: Metal Nanoparticle Structure, and Interaction with the Graphene-Structured Substrate Surface, Langmuir. 26 (2010) 3807–3814.
[53] K.S. Habicht, D.E. Canfield, Sulfur isotope fractionation during bacterial sulfate reduction in organic-rich sediments, Geochim. Cosmochim. Acta. 61 (1997) 5351–5361.
[54] A.G. Harrison, H.G. Thode, The kinetic isotope effect in the chemical reduction of sulphate, Trans. Faraday Soc. 53 (1957) 1648.
[55] N.T. Kita, T. Ushikubo, B. Fu, J.W. Valley, High precision SIMS oxygen isotope analysis and the effect of sample topography, Chem. Geol. 264 (2009) 43–57.
[56] N.T. Kita, J.M. Huberty, R. Kozdon, B.L. Beard, J.W. Valley, High-precision SIMS oxygen, sulfur and iron stable isotope analyses of geological materials: accuracy, surface topography and crystal orientation, Surf. Interface Anal. 43 (2011) 427–431.